© 2013 Science Wise Publishing & DE GRUYTER DOI 10.1515/nanoph-2012-0032SUP — Nanophotonics 2013; 2(2): Ad1–Ad3

Søren Raza[a], Nicolas Stenger[a], Shima Kadkhodazadeh, Søren V. Fischer, Natalie Kostesha, Antti-Pekka Jauho, Andrew Burrows, Martijn Wubs and N. Asger Mortensen*

Supplemental data

1 Shape analysis

The diameters of our nanoparticles are determined by using the free online image analysis tool ImageJ [1] which includes a particle analysis package. We use the 2D images taken in STEM mode to measure the surface area A of the nanoparticle, whereafter we determine the mean nanoparticle diameter D using the relation $A=\pi(D/2)^2$. The particle analysis tool also evaluates the maximum D_{max} and minimum D_{min} diameters of the nanoparticle and the difference between these two diameters, i.e., $\Delta D=D_{max}-D_{min}$ provides us a measure for error in the nanoparticle diameter (shown as the error bar in Article Figure 2). The relative size error ($\Delta D/D$) then represents the deviation of the shape of the particles from a perfect circle.

Supplementary Figure 1 displays a histogram with the number of particles as function of the relative size error (5% interval between each bar). The first observation is that the relative error in the diameter is spread from 5% to 50% with a maximum of counts centered on 15% deviation. We also see that more than 70% of the particles have an error smaller than 20%, thus giving us confidence that assuming the particles to be spherical is justified. We also emphasize that this analysis was made on 2D images which are the projections of the 3D shapes of the nanoparticles onto the plane parallel to the substrate. This lack of information in the third dimension leaves indeterminacy of the exact shape of the particle. However, since the nanoparticles are fabricated in a liquid phase suspension [2], i.e., growing identically in three dimensions, we can to a first approximation infer that we have the same relative size error distribution in the third dimension perpendicular to the substrate, thus assuming that particle orientation is independent of its shape deformation.

In order to understand the scattering of the SP resonance energies observed in Article Figure 2, we model the deviation from the perfect spherical shape as an ellipsoidal particle with minor and major axes. We calculate the optical polarizability of two different types of ellipsoids: the prolate spheroid (one major and two equal minor axes) and the oblate spheroid (two equal major and one minor axes). The polarizability is calculated within the local Drude theory under two different polarizations of the incident electric field, parallel to the major axis or parallel to the minor axis [3]. The perfect spherical sphere is deformed while keeping the volume constant. We use a relative deformation of the major (minor) axis of 20%

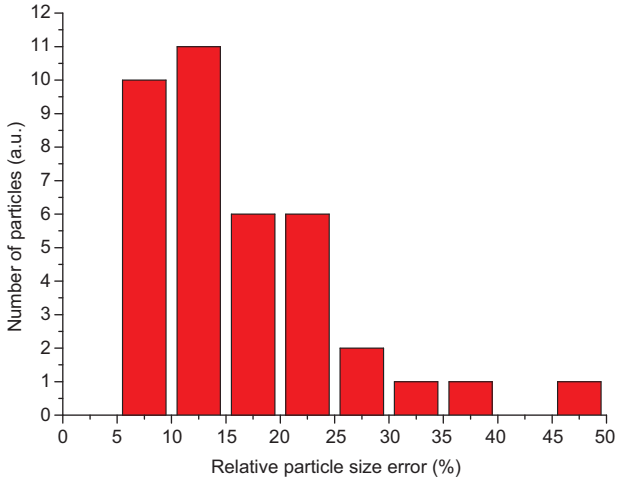

Supplementary Figure 1 Histogram showing the distribution of relative size error $\Delta D/D$. The relative size error represents the shape deviation of the nanoparticle from a perfect circle in the 2D STEM image.

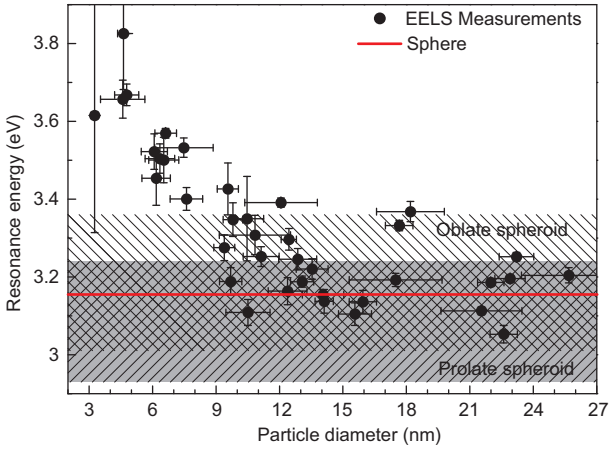

Supplementary Figure 2 Local-response calculations of the SP resonance for perfectly spherical (red line), oblate (white patterned) and prolate (gray patterned) particles under excitation of different polarizations.

for the prolate (oblate) particles which corresponds to the deviation of the majority of the nanoparticles studied.

The results are shown in Supplementary Figure 2. The red line represents the local Drude calculation for a perfect sphere (same as Article Figure 2). The gray patterned area corresponds to the span of resonance energies for the prolate particles, when a relative deviation of the major axis of 20% is allowed. The part of the area that is above the red line (i.e., blueshifted with respect to the perfect sphere) corresponds to a polarization along the minor axis, while the part below the red line (i.e., redshifted with respect to the perfect sphere) is due a polarization along the major axis. For the polarization along the minor axis, we see a blueshift of approximately 0.1 eV of the SP resonance while we obtain a redshift of approximately 0.2 eV for the polarization along the major axis. The increased redshift observed for the polarization along the major axis is due to the fact that a size increase of 20% on the major axis will give only a size decrease of 9% on the minor axis (scales as $1/a_{\mathrm{major}}^2$, where a_{major} is the length of the major axis) for a constant volume. The same arguments are valid for the oblate case with the exception that here the blueshift is higher than the redshift (major and minor axes are inverted). However, the overall span of resonance energies considering both type of spheroids is approximately 0.4 eV. Interestingly, this interval is similar to the scattering of the resonance energy observed in Article Figure 2 for particles above 10 nm, where the local theory is still valid. However, we emphasize that the measured resonance energies for the smallest particles (below 10 nm) exceeds this span of resonance energies, and thus the observed blueshift cannot be explained by a simple shape deviation argument.

In conclusion, we see that the deviation from the spherical shape into ellipsoid-like particles and the thereby prompted dependency on the location of the EELS probe when measuring the SP resonance gives a reasonable and probable explanation for the spread but not for the magnitude of SP resonance energies observed in our measurements.

2 Substrate effects: dipole-dipole interaction

The optical polarizability α of a single sphere in a homogeneous background ε_{B} can be modified to take into account the presence of a semi-infinite substrate with permittivity ε_{S} using a simple image charge model. In this picture, the coupling between the sphere and the substrate is based on a dipole-dipole interaction between the dipole moment of the sphere and the weaker dipole moment of the image charges in the substrate. Taking only dipole moments into account is an approximation. Due to the symmetry-breaking presence of the substrate, there are two separate cases to be treated for the direction of the incident field: one when the incident electric field is parallel to the substrate, the other when the incident field is perpendicular to the substrate. It has been shown that the altered polarizability α_{sub} in the presence of the semi-infinite substrate is [4–6]

$$\alpha_{\mathrm{sub}}=\alpha\left[1-\frac{\kappa\alpha}{4\pi(2R)^3}\frac{\varepsilon_{\mathrm{S}}-\varepsilon_{\mathrm{B}}}{\varepsilon_{\mathrm{S}}+\varepsilon_{\mathrm{B}}}\right]^{-1}, \tag{S1}$$

where κ=-1 for a parallel incident electric field while κ=2 for a perpendicular electric field. The interesting case for our EELS measurements is when κ=2, since the electric field produced by a swift electron is predominantly in the same direction as the movement of the electron, i.e., perpendicular to the substrate.

Supplementary Figure 3 shows calculations on the SP resonance energy performed using Eq. (S1) with $\varepsilon_{\mathrm{S}}=2.08^2$ and $\varepsilon_{\mathrm{B}}=1$. Ellipsometry measurements of the complex refractive index $n=n'+in''$ on the Si_3N_4 substrate has been provided by the manufacturer of the TEM membranes (TEMwindows.com), showing an almost constant index of refraction of $n'\approx 2.08$ and a negligible extinction coefficient $n''\approx 0$ in the energy range we consider (3.0–3.9 eV). The provided measurements are very similar to that of Ref. [7]. We emphasize that with the dipole-dipole model for the substrate no fitting of the background permittivity has been done.

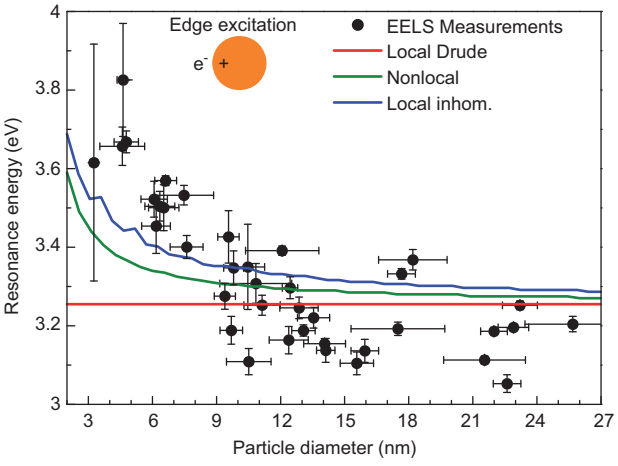

Supplementary Figure 3 The same as Article Figure 2, but calculated using Eq. (S1) with κ=2, $\varepsilon_{\mathrm{S}}=2.08^2$ and $\varepsilon_{\mathrm{B}}=1$.

Supplementary Figure 3 shows that the dipole-dipole interaction predicts a slightly larger resonance energy in the classical limit (i.e., for the largest particles) compared to the fitted homogeneous background permittivity approach used for Article Figure 2. However, the blueshift in the resonance energy for decreasing particle size in the two semiclassical models is very similar to the effective homogeneous background approach, and thus the dipole-dipole model for the substrate cannot fully account for the significantly larger experimental blueshift. We also see that many of the EELS measurements of the larger particles ($2R$>10 nm) lie at lower resonance energies than predicted by any of the theoretical substrate models. These discrepancies suggest that the simple dipole-dipole model for the substrate is inadequate to describe our experimental observations, and that a complete understanding of the effect of the substrate requires the inclusion of higher-order multipoles and the finite thickness of the substrate [8, 9].

References

[1] Available at: http://imagej.nih.gov/ij/.
[2] Mulfinger L, Solomon SD, Bahadory M, Jeyarajasingam A, Rutkowsky SA, Boritz C. Synthesis and study of silver nanoparticles. J Chem Educ 2007;84:322–5.
[3] Maier SA. Plasmonics: fundamentals and applications. New York: Springer; 2007.
[4] Yamaguchi T, Yoshida S, Kinbara A. Optical effect of the substrate on the anomalous absorption of aggregated silver films. Thin Solid Films 1974;21:173–87.
[5] Jain PK, Huang W, El-Sayed MA. On the universal scaling behavior of the distance decay of plasmon coupling in metal nanoparticle pairs: a plasmon ruler equation. Nano Lett 2007;7:2080–8.
[6] Novotny L, Hecht B. Principles of nano-optics. New York: Cambridge; 2006.
[7] Bååk T. Silicon oxynitride; a material for GRIN optics. Appl Opt 1982;21:1069–72.
[8] Boardman AD, Paranjape BV. The optical surface modes of metal spheres. J Phys F Met Phys 1977;7:1935.
[9] Ruppin R. Surface modes and optical absorption of a small sphere above a substrate. Surf Sci 1983;127:108–18.